Optimal Reference Tracking with Arbitrary Sampling

Jacob Higgins [a], Alessandro V. Papadopoulos [b], Enrico Bini [c], Nicola Bezzo [a]

[a] *University of Virginia, USA*

[b] *Mälardalen University, Sweden*

[c] *University of Turin, Italy*

Abstract

It is a standard engineering practice to design feedback-based control to have a system follow a given trajectory. While the trajectory is continuous-time, the sequence of references is varied at discrete times, which may not be periodic. In this paper, we propose a method to determine the discrete-time references which minimizes a weighted L^2 distance between the achieved trajectory and the target trajectory. Also, we consider any arbitrary sequence of sampling instants. The proposed method is then assessed over different simulation results, analyzing the design parameters' effects, and over an unmanned aerial vehicle (UAV) use case.

Key words: Mobile robots; optimal control; trajectory tracking.

1 Introduction

The majority of the engineering applications around us utilizes feedback-based control mechanisms. A classic approach is to design a reference signal to be tracked and then regulate control actions to achieve a desired system's behavior. Normally, the desired trajectory is a continuous-time function, since it represents a motion in the physical world. However, the reference fed to the system is in discrete-time, since it is computed by a digital system. Also, standard approaches assume that the discretization of time is periodic. Instead, the method proposed in this paper allows the references to be sampled aperiodically, changing at any time instant and determining the optimal references that minimize the L^2 distance to a given trajectory.

This is a common problem, for example, in robotics applications, where continuous reference trajectories should be followed, while the robot can be controlled only by selecting a discrete set of points – also called *waypoints* – that are used as a discrete reference for the robot. Such points must be selected with care to make the robot follow the actual continuous reference trajectory in a precise way. A natural choice for such waypoints would be to pick them as samples – not necessarily periodic – on the continuous reference trajectory. However, this may not lead to very accurate results. Figure 1 shows a scenario where a mobile robot is given a continuous trajectory to follow but can only utilize a finite number of waypoints (five in this instance) to approximate it. Sampling the waypoints on the reference trajectory (top graph) results in a significant tracking error. The focus of this paper is to investigate the formulation of discrete-time references to minimize tracking errors and enable optimal tracking of the original continuous trajectory. The results obtained with the proposed approach are shown in the bottom graph of Figure 1.

The usage of sampled-data techniques for the control of linear systems is virtually ubiquitous, thanks to the flexibility given by the adoption of digital implementations of the control system (Alur et al., 2007; Chen and Francis, 2012; Ragazzini and Franklin, 1958). However, even if sampled-data techniques provide several advantages, the digital implementation sets limitations and constraints on the information available for feedback (Seron et al., 2012).

In the past, similar problems have been addressed by designing $\mathcal{H}_2$ or $\mathcal{H}_\infty$ hybrid control systems (Chen and Francis, 1995; Geromel et al., 2019; Hara et al., 1994). Most of these approaches focus on the solution of optimal and robust control problems via convex optimization methods whose constraints are expressed by

Email addresses: jdh4je@virginia.edu (Jacob Higgins), alessandro.papadopoulos@mdu.se (Alessandro V. Papadopoulos), enrico.bini@unito.it (Enrico Bini), nbezzo@virginia.edu (Nicola Bezzo).

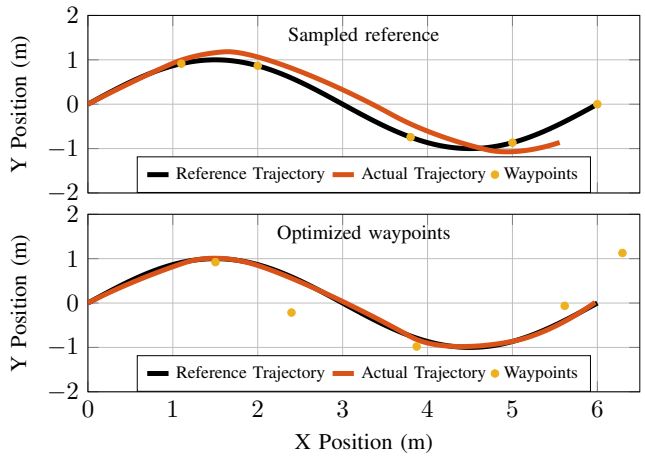

Fig. 1. Illustrative example.

LMIs (Boyd et al., 1994), that ensure the optimal performance (Geromel and Souza, 2015). However, such approaches mostly focus on the optimal design of the digital controller. In this paper, we focus instead on the computation of the optimal reference signal in the discrete-time given a desired trajectory of the system output, assuming that a control loop system has been designed. The proposed approach is simpler than other approaches, e.g., Geromel et al. (2019); Geromel and Souza (2015), as it provides a closed-form solution without solving an optimization problem. Also, our problem cannot be cast as a standard optimal sampled-time LQR design (Anderson and Moore, 2007; Levis et al., 1971) as we exploit the explicit information of the future trajectory to be tracked.

The generation of a discrete-time reference signal can be thought of as similar to the problem of waypoint generation in robotics systems (Hildebrandt et al., 2020; Hwang et al., 2003; Lau et al., 2009; Liu and Sun, 2014; Mellinger and Kumar, 2011; Penicka and Scaramuzza, 2022). Practical applications range from mobile robotics where waypoints are three-dimensional positions in space (Wang et al., 2020) to robotic manipulators that use waypoints defined within a more general state space (Yang et al., 2021). In fact, the definition of waypoints implicitly defines a timing law of the reference trajectory. For example, in the UAV context, optimization-based techniques have been used to find the trajectory in cluttered environments while being robust to communication losses (Higgins et al., 2022). The contribution of this paper is inspired by this waypoint generation problem, but it abstracts from it, providing a more general solution.

This paper extends our preliminary work in (Bini et al., 2022) by proposing the following new contributions:

(1) We analytically determine a closed-form solution for the optimal references that minimize a quadratic cost, allowing the references to vary at arbitrary sampling instants (in Section 4);
(2) We extend the closed-form solution to the case accounting for an additional quadratic cost due to the reference signal (in Section 5).

2 Preliminaries and System Model

In this work, the symbol $^\top$ postfixed to vectors or matrices denotes their transpose. The symbols $\mathbb{R}$, $\mathbb{R}_+$, and $\mathbb{N}$ denote the sets of real, non-negative real, and natural numbers, respectively. Vector variables are indicated with bold fonts, e.g., $\boldsymbol{x}$. The 2-norm of any vector $\boldsymbol{x} \in \mathbb{R}^n$ is denoted by $\|\boldsymbol{x}\| = \sqrt{\boldsymbol{x}^\top \boldsymbol{x}}$. For any linear operator $\mathcal{L}$, we denote its null space (or *kernel*) by $\ker \mathcal{L}$ that is $\boldsymbol{x} \in \ker \mathcal{L} \;\Leftrightarrow\; \mathcal{L}\boldsymbol{x} = 0$. Finally, we use $f \circ g$ to denote the composition of functions, that is $f \circ g(x) = f(g(x))$.

The system has an internal controller which is designed so that the output $\boldsymbol{y}(t)$ follows a given reference $\boldsymbol{r}(t)$ (represented by the block "Closed-loop Continuous-time Dynamics" in Figure 2). The internal continuous-time linear time-invariant dynamics of the system are given by

$$\begin{aligned} \dot{\boldsymbol{x}}(t) &= A\boldsymbol{x}(t) + B\boldsymbol{r}(t) \\ \boldsymbol{y}(t) &= C\boldsymbol{x}(t), \end{aligned} \tag{1}$$

with

- an internal *state* $\boldsymbol{x}(\cdot) : \mathbb{R}_+ \mapsto \mathbb{R}^n$,
- a *reference* function $\boldsymbol{r}(\cdot) : \mathbb{R}_+ \mapsto \mathbb{R}^m$, to be followed, and
- the system *output* $\boldsymbol{y}(\cdot) : \mathbb{R}_+ \mapsto \mathbb{R}^p$.

We remark that despite $\boldsymbol{r}(t)$ and $\boldsymbol{y}(t)$ normally having images in the same space, we keep them separate as our analysis can address the more general case. We assume that the state $\boldsymbol{x}(t)$ of the system is observable.

The internal state is sampled at the sampling instants in $\{t_k\}_{k\in\mathbb{N}}$ and the sampled state is denoted by $\boldsymbol{x}(t_k) = \boldsymbol{x}_k$. The sampling instants are constant and only in Section 4.1 we address the optimization of them. We conveniently denote the separation to the next sampling instant by $\tau_k = t_{k+1} - t_k$. The reference is held constant during every interval $[t_k, t_{k+1})$, that is

$$\forall k,\ \forall t \in [t_k, t_{k+1}), \quad \boldsymbol{r}(t) = \boldsymbol{r}_k \tag{2}$$

with $\boldsymbol{r}_k \in \mathbb{R}^m$ being the constant reference applied over the k-th interval. We remark once again that we are allowing non-periodic sampling, i.e. τ_k may vary with k.

To analyze the dynamics of (1) in the presence of a reference $\boldsymbol{r}_k$ held constant for an interval of duration τ_k, we discretize it over the interval $[t_k, t_{k+1})$. For this purpose,

we define

$$\Phi(t) = e^{At}, \qquad \bar{A}_{k_1,k_0} = \Phi(t_{k_1} - t_{k_0}) \quad (3)$$

$$\Gamma(t) = \int_0^t e^{A(t-s)}\, ds\, B, \qquad \bar{B}_k = \Gamma(\tau_k). \quad (4)$$

Standard properties of $\Phi(t)$ and $\Gamma(t)$ that we may be using later on are that

$$\bar{A}_{k,k} = \Phi(t_k - t_k) = e^{A0} = I$$
$$\Gamma(0) = 0.$$

With these notations, the evolution of the state $\boldsymbol{x}$ as a function of time can be written as

$$\boldsymbol{x}_k = \bar{A}_{k,0}\boldsymbol{x}_0 + \sum_{i=0}^{k-1} \bar{A}_{k,i+1}\bar{B}_i\, \boldsymbol{r}_i$$
$$\forall k, \forall t \in [t_k, t_{k+1}) \quad \boldsymbol{x}(t) = \Phi(t - t_k)\boldsymbol{x}_k + \Gamma(t - t_k)\boldsymbol{r}_k. \quad (5)$$

3 Trajectory Tracking: The Problem

The goal of this work is to determine the optimal references $\boldsymbol{r}_k$ such that the output $\boldsymbol{y}(t)$ of the system follows *as close as possible* a given target trajectory $\tilde{\boldsymbol{y}}(t)$. Figure 2 shows a blocks diagram, in which:

- the inputs of our "Reference Generator" are:
  - the continuous-time target trajectory $\tilde{\boldsymbol{y}}(t)$ and
  - the sampled state $\boldsymbol{x}_k$, while
- the output is the reference $\boldsymbol{r}_k$, which is then fed to the system after ZOH.

Let us now formally define the necessary notions and notations to properly state the problem. The *target trajectory* is modeled by a function $\tilde{\boldsymbol{y}}(\cdot) : \mathbb{R}_+ \mapsto \mathbb{R}^p$, which has image in the same set $\mathbb{R}^p$ of the output $\boldsymbol{y}$.

The distance between the target trajectory $\tilde{\boldsymbol{y}}$ and the achieved output trajectory $\boldsymbol{y}$ is modeled by the norm

$$\int_I e^{-\beta t} \|\tilde{\boldsymbol{y}}(t) - \boldsymbol{y}(t)\|^2 dt$$

with the integration interval I depending on the specific characteristics of the problem, and the weight $e^{-\beta t}$ introduced to give a relative importance to the near or far future. Notice that by setting $\beta = 0$, the norm is the standard L^2 norm.

We denote with $t_{k'}$ the instant at which the system state $\boldsymbol{x}(t_{k'})$ is sampled and a new reference $\boldsymbol{r}_{k'}$ is set and held constant over the interval $[t_{k'}, t_{k'+1})$. Also, we consider the integration interval $[t_{k'}, t_{k'+N})$, where N is the number of future references $\boldsymbol{r}_k$ that should be computed.

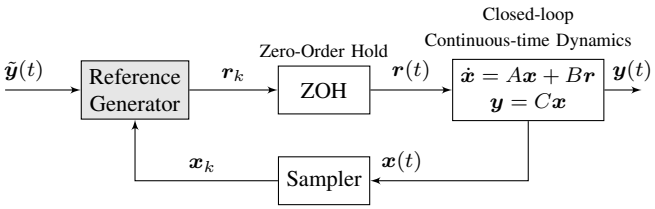

Fig. 2. Control scheme of our approach.

Finally, to have more compact and insightful expressions we introduce the following *inner product* between any pair of functions $f, g : \mathbb{R} \to \mathbb{R}^p$ with image in the output space

$$\langle f, g \rangle_{\beta,[a,b]} = \int_a^b e^{-\beta(t-a)} f^\top(t) g(t)\, dt, \quad (6)$$

and the induced norm

$$\|f\|_{\beta,[a,b]} = \sqrt{\langle f, f \rangle_{\beta,[a,b]}} = \sqrt{\int_a^b e^{-\beta(t-a)} \|f(t)\|^2\, dt}, \quad (7)$$

When the left boundary of the interval of integration is $a = 0$, we use the shortcut notations

$$\langle f, g \rangle_{\beta,[0,b]} = \langle f, g \rangle_{\beta,b}\,, \qquad \|f\|_{\beta,[0,b]} = \|f\|_{\beta,b}\,.$$

Having introduced these concepts and notations, we define the optimal references $(\boldsymbol{r}_{k'}, \ldots, \boldsymbol{r}_{k'+N-1})$ as the solution that minimizes the following cost

$$\min_{(\boldsymbol{r}_{k'}, \ldots, \boldsymbol{r}_{k'+N-1})} \|\tilde{\boldsymbol{y}} - \boldsymbol{y}\|^2_{\beta,[t_{k'}, t_{k'+N}]}\,. \quad (8)$$

4 Trajectory Tracking: The Solution

In this section, we develop the solution to the problem of minimizing the cost of (8). To simplify the mathematics, in this section we are going to assume that the index k' of the instant when setting the reference is equal to zero, that is, $k' = 0$, and that $t_{k'} = t_0 = 0$.

First, we re-write the cost of (8) as

$$J = \sum_{k=0}^{N-1} e^{-\beta t_k} \underbrace{\|\tilde{\boldsymbol{y}} \circ \Delta_k - C\Phi\boldsymbol{x}_k - C\Gamma\boldsymbol{r}_k\|^2_{\beta,\tau_k}}_{J_k} \quad (9)$$

by exploiting elementary properties of the inner product of (6). In (9), $\Delta_k(t) = t + t_k$ denotes a backward translation over time by t_k, and J_k denotes the contribution to the cost J when integrating over the k-th interval $[t_k, t_{k+1})$.

By replacing in (9), the state $\boldsymbol{x}_k$ with its explicit expression of (5), we get

$$J_k = \left\| \tilde{\boldsymbol{y}} \circ \Delta_k - C\Phi \bar{A}_{k,0} \boldsymbol{x}_0 - C\Pi_k \boldsymbol{r} \right\|^2_{\beta,\tau_k} \tag{10}$$

with $\boldsymbol{r} = (\boldsymbol{r}_0, \ldots, \boldsymbol{r}_{N-1}) \in \mathbb{R}^{mN}$ representing more compactly all the N references. The mapping $\Pi_k : \mathbb{R} \to \mathcal{L}(\mathbb{R}^{mN}, \mathbb{R}^n)$ returns for every value of t a linear map $\Pi_k(t) : \mathbb{R}^{mN} \to \mathbb{R}^n$. The map $\Pi_k(t)$ represents the impact of all the N references of $\boldsymbol{r}$ onto the state $\boldsymbol{x}(t)$ over the k-th interval $[t_k, t_{k+1})$. The map Π_k is linear and is defined by the following matrix in $\mathbb{R}^{n \times mN}$

$$\Pi_k = \Bigg[\overbrace{\Phi \bar{A}_{k,1} \bar{B}_0}^{\text{multiply } \boldsymbol{r}_0} \quad \overbrace{\Phi \bar{A}_{k,2} \bar{B}_1}^{\text{multiply } \boldsymbol{r}_1} \cdots \\ \cdots \underbrace{\Phi \bar{A}_{k,k-1} \bar{B}_{k-2}}_{\boldsymbol{r}_{k-2}} \underbrace{\Phi \bar{B}_{k-1}}_{\boldsymbol{r}_{k-1}} \underbrace{\Gamma}_{\boldsymbol{r}_k} \underbrace{0}_{\boldsymbol{r}_{k+1}} \cdots \underbrace{0}_{\boldsymbol{r}_{N-1}} \Bigg] \tag{11}$$

so that

$$\Pi_k(t)\boldsymbol{r} = \Phi(t) \sum_{i=0}^{k-1} \bar{A}_{k,i+1} \bar{B}_i \, \boldsymbol{r}_i + \Gamma(t) \boldsymbol{r}_k.$$

The definition of each of the N blocks of Π_k, each one of size $n \times m$, reveals that:

- The block multiplying $\boldsymbol{r}_k$ is set to Γ, which represents the impact of $\boldsymbol{r}_k$ over the k-th interval itself,
- If $i > k$, then the i-th $n \times m$ block of Π_k multiplying $\boldsymbol{r}_i$ is set to 0 to represent the fact that future references $\boldsymbol{r}_i$ cannot have an impact on the k-th interval,
- If $i < k$, $\boldsymbol{r}_i$ is multiplied by $\Phi \bar{A}^{k-i-1} \bar{B}_i$ to account for the impact of the past reference $\boldsymbol{r}_i$ onto the k-th interval.

The cost J_k of (10) is quadratic in $\boldsymbol{r}$ and by isolating each term by the degree of the dependency on $\boldsymbol{r}$, we get

$$\begin{aligned} J_k &= \left\| \tilde{\boldsymbol{y}} \circ \Delta_k - C\Phi \bar{A}_{k,0} \boldsymbol{x}_0 - C\Pi_k \boldsymbol{r} \right\|^2_{\beta,\tau_k} \\ &= \left\| \tilde{\boldsymbol{y}} \circ \Delta_k - C\Phi \bar{A}_{k,0} \boldsymbol{x}_0 \right\|^2_{\beta,\tau_k} && \text{(constant)} \\ &\quad - 2 \left\langle \tilde{\boldsymbol{y}} \circ \Delta_k - C\Phi \bar{A}_{k,0} \boldsymbol{x}_0, C\Pi_k \boldsymbol{r} \right\rangle_{\beta,\tau_k} && \text{(linear)} \\ &\quad + \left\| C\Pi_k \boldsymbol{r} \right\|^2_{\beta,\tau_k} && \text{(quadratic).} \end{aligned}$$

The inner product of the second linear term can be written as a more explicit linear function of $\boldsymbol{r}$ by

$$\left\langle \tilde{\boldsymbol{y}} \circ \Delta_k - C\Phi \bar{A}_{k,0} \boldsymbol{x}_0, C\Pi_k \boldsymbol{r} \right\rangle_{\beta,\tau_k} = \tilde{\boldsymbol{Y}}_k \boldsymbol{r} - \boldsymbol{x}_0^\top \boldsymbol{V}_k \boldsymbol{r}$$

with $\tilde{\boldsymbol{Y}}_k \in \mathbb{R}^{1 \times mN}$ accounting for the target trajectory in the k-th interval $[t_k, t_{k+1})$ and defined by

$$\tilde{\boldsymbol{Y}}_k = \left[\tilde{\boldsymbol{Y}}_{\Phi,k} \bar{A}_{k,1} \bar{B}_0 \cdots \tilde{\boldsymbol{Y}}_{\Phi,k} \bar{B}_{k-1} \tilde{\boldsymbol{Y}}_{\Gamma,k} 0 \cdots 0 \right] \tag{12}$$

$$\tilde{\boldsymbol{Y}}_{\Phi,k} = \left\langle \tilde{\boldsymbol{y}} \circ \Delta_k, C\Phi \right\rangle_{\beta,\tau_k} \tag{13}$$

$$\tilde{\boldsymbol{Y}}_{\Gamma,k} = \left\langle \tilde{\boldsymbol{y}} \circ \Delta_k, C\Gamma \right\rangle_{\beta,\tau_k} \tag{14}$$

and $\boldsymbol{V}_k \in \mathbb{R}^{n \times mN}$, expressing the impact of the initial state $\boldsymbol{x}_0$ over the k-th interval, defined by

$$\boldsymbol{V}_k = \bar{A}_{k,0}^\top \big[M_{\Phi\Phi,k} \bar{A}_{k,1} \bar{B}_0 \cdots M_{\Phi\Phi,k} \bar{B}_{k-1} \\ M_{\Phi\Gamma,k} \; 0 \cdots 0 \big] \tag{15}$$

$$M_{\Phi\Phi,k} = \left\langle C\Phi, C\Phi \right\rangle_{\beta,\tau_k} \tag{16}$$

$$M_{\Phi\Gamma,k} = \left\langle C\Phi, C\Gamma \right\rangle_{\beta,\tau_k} \tag{17}$$

Finally, the quadratic term $\|C\Pi_k(t)\boldsymbol{r}\|^2_{\beta,\tau_k}$ of J_k is expanded as follows

$$\|C\Pi_k \boldsymbol{r}\|^2_{\beta,\tau_k} = \left\langle C\Pi_k \boldsymbol{r}, C\Pi_k \boldsymbol{r} \right\rangle_{\beta,\tau_k} = \boldsymbol{r}^\top \boldsymbol{Q}_k \boldsymbol{r}. \tag{18}$$

The quadratic form $\boldsymbol{r}^\top \boldsymbol{Q}_k \boldsymbol{r}$ can also be written more expressively through all its $N \times N$ blocks $\boldsymbol{Q}_k[i,j]$ of size $m \times m$. Each block $\boldsymbol{Q}_k[i,j] \in \mathbb{R}^{m \times m}$ is left-multiplied by $\boldsymbol{r}_i^\top$ and right-multiplied by $\boldsymbol{r}_j$. Formally, we can write:

$$\boldsymbol{r}^\top \boldsymbol{Q}_k \boldsymbol{r} = \sum_{i=0}^{N-1} \sum_{j=0}^{N-1} \boldsymbol{r}_i^\top \boldsymbol{Q}_k[i,j] \boldsymbol{r}_j$$

with all blocks $\boldsymbol{Q}_k[i,j] \in \mathbb{R}^{m \times m}$ indexed by $i, j = 0, \ldots, N-1$ and defined by

$$\begin{cases} \boldsymbol{Q}_k[i,j] = \bar{B}_i^\top \bar{A}_{k,i+1}^\top M_{\Phi\Phi,k} \bar{A}_{k,j+1} \bar{B}_j & i \le j < k \\ \boldsymbol{Q}_k[i,k] = \bar{B}_i^\top \bar{A}_{k,i+1}^\top M_{\Phi\Gamma,k} & i < k \\ \boldsymbol{Q}_k[k,k] = M_{\Gamma\Gamma,k} & \\ \boldsymbol{Q}_k[i,j] = \boldsymbol{Q}_k[j,i]^\top & j \le i \le k \\ \boldsymbol{Q}_k[i,j] = \boldsymbol{0} & i > k \;\vee\; j > k. \end{cases} \tag{19}$$

The definition of $\boldsymbol{Q}_k$ in (19) exploits the definitions of $M_{\Phi\Phi,k}$, $M_{\Phi\Gamma,k}$ of Eqs. (16) and (17) respectively, and $M_{\Gamma\Gamma,k}$ defined by

$$M_{\Gamma\Gamma,k} = \left\langle C\Gamma, C\Gamma \right\rangle_{\beta,\tau_k}. \tag{20}$$

The final derivation of $\boldsymbol{Q}_k$ allows us to write the cost J_k accumulated in the k-th interval as

$$J_k = \left\| \tilde{\boldsymbol{y}} \circ \Delta_k - C\Phi \bar{A}^k \boldsymbol{x}_0 \right\|^2_{\beta,\tau_k} - 2(\tilde{\boldsymbol{Y}}_k - \boldsymbol{x}_0^\top \boldsymbol{V}_k)\boldsymbol{r} + \boldsymbol{r}^\top \boldsymbol{Q}_k \boldsymbol{r} \tag{21}$$

and then to state the following theorem which offers the explicit expression of the cost J.

Theorem 1 *The cost J of Equation (9) is equal to*

$$J = \text{const.} - 2(\tilde{\boldsymbol{Y}} - \boldsymbol{x}_0^\top \boldsymbol{V})\boldsymbol{r} + \boldsymbol{r}^\top \boldsymbol{Q}\boldsymbol{r} \tag{22}$$

with:

- $\text{const.} = \sum_{k=0}^{N-1} e^{-\beta t_k} \left\| \tilde{\boldsymbol{y}} \circ \Delta_k - C\Phi \bar{A}^k \boldsymbol{x}_0 \right\|^2_{\beta,\tau_k}$
- $\tilde{\boldsymbol{Y}} = \sum_{k=0}^{N-1} e^{-\beta t_k} \tilde{\boldsymbol{Y}}_k$
- $\boldsymbol{V} = \sum_{k=0}^{N-1} e^{-\beta t_k} \boldsymbol{V}_k$
- $\boldsymbol{Q} = \sum_{k=0}^{N-1} e^{-\beta t_k} \boldsymbol{Q}_k$

Proof: The expression of (22) follows from (9) and from each of the costs J_k of (21) properly weighted.

Theorem 1 states that the cost, as initially defined by (9) is a quadratic form in $\boldsymbol{r}$. The determination of the optimal $\boldsymbol{r}$ that minimizes such a cost, however, depends on the characteristics of the linear and the quadratic terms of (22).

Lemma 1 (Lemma 1 in Bini et al. (2022)) *The matrix $\boldsymbol{Q} \in \mathbb{R}^{mN \times mN}$ is:*

- *symmetric, and*
- *positive semi-definite.*

The matrix $\boldsymbol{Q}$, however, not be strictly positive definite. The next lemma provides some insights about the null space of $\boldsymbol{Q}$ so that we can find the minimum of the cost of (22).

Lemma 2 (Lemma 2 in Bini et al. (2022)) *If $\boldsymbol{r} \in \ker \boldsymbol{Q}$ then $\boldsymbol{r} \in \ker(\tilde{\boldsymbol{Y}} - \boldsymbol{x}_0^\top \boldsymbol{V})$.*

Lemma 1 states that $\boldsymbol{Q}$ is positive semi-definite and symmetric. Hence it can be diagonalized as follows:

$$\begin{bmatrix} \Lambda & 0 \\ 0 & 0 \end{bmatrix} = \begin{bmatrix} H^\top \\ H_0^\top \end{bmatrix} \boldsymbol{Q} \begin{bmatrix} H & H_0 \end{bmatrix}$$

with:

- Λ the diagonal matrix with the strictly positive eigenvalue of $\boldsymbol{Q}$,
- $\begin{bmatrix} H & H_0 \end{bmatrix}$ the orthonormal matrix which diagonalizes $\boldsymbol{Q}$,
- the columns of H_0 are an orthonormal basis of $\ker \boldsymbol{Q}$, and
- the columns of H are an orthonormal basis of the subspace of $\mathbb{R}^{mN}$ orthogonal to $\ker \boldsymbol{Q}$.

Algorithm 1 Optimizing the sampling instants

Input: $\boldsymbol{t}_{\text{per}}$: Periodic sampling, $\tilde{\boldsymbol{y}}$: Target trajectory, *maxIter*: Maximum number of iterations.
Output: $\boldsymbol{t}^*$: Optimized sampling instants, $\boldsymbol{r}^*$: Optimal references.

```
t ← t_per
J* ← +∞
i ← 0
while i < maxIter do
    r, J ← optRefs(t, ỹ) {Eqs. (24)-(25)}
    if J < J* then
        t* ← t
        r* ← r
    end if
    t ← samplingOptimStep(t, ỹ, r)
    i ← i + 1
end while
return t*, r*;
```

Following the same steps as in Bini et al. (2022), we find that the space of all solutions is

$$\{\boldsymbol{r}^*\} + \text{span}\, H_0 = \{\boldsymbol{r}^* + \boldsymbol{v} : \boldsymbol{v} \in \text{span}\, H_0\} \tag{23}$$

with

$$\boldsymbol{r}^* = H\Lambda^{-1}H^\top(\tilde{\boldsymbol{Y}}^\top - \boldsymbol{V}^\top \boldsymbol{x}_0). \tag{24}$$

By replacing the optimal solution $\boldsymbol{r}^*$ in the cost, we can find the minimal cost J^*, that is

$$J^* = \sum_{k=0}^{N-1} e^{-\beta t_k} \left\| \tilde{\boldsymbol{y}} \circ \Delta_k - C\Phi \bar{A}^k \boldsymbol{x}_0 \right\|^2_{\beta,\tau_k} - (\tilde{\boldsymbol{Y}} - \boldsymbol{x}_0^\top \boldsymbol{V})H\Lambda^{-1}H^\top(\tilde{\boldsymbol{Y}}^\top - \boldsymbol{V}^\top \boldsymbol{x}_0). \tag{25}$$

4.1 Computing the Aperiodic Sampling Instants

Thus far, we have considered the aperiodic sampling instants $\boldsymbol{t} = \{t_0, t_1, \ldots, t_{N-1}, t_N\}$ as known. However, we can indeed formulate an optimization problem on the variables $\boldsymbol{t}$ that minimizes the cost function (22), subject to the constraint that $t_N - t_0 = T$, which is the length of the horizon. Unfortunately, such an optimization problem is not convex, and the computation of the optimal sampling instants $\boldsymbol{t}$ may not be always possible. Optimal sampling was investigated by Bini and Buttazzo (2014) in the context of aperiodic LQR cost. However, the same techniques do not seem to be directly applicable to our case.

Different global optimization techniques (Clerc and Kennedy, 2002; Ugray et al., 2007) can be used to compute sub-optimal solutions. One possible way of optimizing over the sampling instants is presented in

Algorithm 1. The algorithm starts from the periodic sampling $\boldsymbol{t}_{\text{per}}$, as initial guess. Then, at each iteration, it performs a step toward a possibly better solution (line 10). If such a new solution is lowering the cost, then the current one is updated. Note that the optimization strategy fixes the initial and final points t_0 and t_N, and optimizes the placement of the remaining points, subject to the constraint that all points are monotonically increasing, i.e., $t_i < t_{i+1}$ for all $i = 0, \dots, N-1$. Convergence is guaranteed by updating the solution only if the cost is reduced.

We remark that the implemented algorithm allows any possible choice for taking a step over the solution space. For example, later in Section 6 we use Particle Swarm Optimization.

5 Reference Regularization

Although the references belonging to the affine space of (23) are all optimal, in practice, the positive semi-definite matrix $\boldsymbol{Q}$ may be poorly conditioned (with minimum and maximum non-zero eigenvalues differing by orders of magnitude). This may give rise to references with very large values. For real-world systems, the closed-loop dynamics (1) may not be valid for such large references. For example, large references may lead to large input actuation, which in turn could violate system actuation limits. One common method to mitigate such concerns is to include a regularization term within the cost function that penalizes large values for the decision variable. This paper proposes a modification to the cost (8) that includes a term that additionally penalizes the L^2 norm of the references $\boldsymbol{r}(t)$, that is we aim at minimizing

$$\min_{(\boldsymbol{r}_{k'}, \dots, \boldsymbol{r}_{k'+N-1})} \|\tilde{\boldsymbol{y}} - \boldsymbol{y}\|^2_{\beta,[t_{k'}, t_{k'+N}]} + \alpha \|\boldsymbol{r}(t)\|^2_{0,[t_{k'}, t_{k'+N}]}. \tag{26}$$

with α denoting a relative weight that we are applying to such an additional cost. Thus, this modified cost seeks to balance minimizing both the trajectory error and the reference power. Additionally, this new term is already quadratic in $\boldsymbol{r}(t)$, which makes it suitable for the quadratic minimization of the cost function presented in (22). To explore the implications of including such regularization, we provide the following Lemma.

Lemma 3 *The modified cost of* (26) *may be rewritten as*

$$J = \text{const.} - 2(\tilde{\boldsymbol{Y}} - \boldsymbol{x}_0^\top \boldsymbol{V})\boldsymbol{r} + \boldsymbol{r}^\top \boldsymbol{Q}_{\text{reg}} \boldsymbol{r} \tag{27}$$

with

$$\boldsymbol{Q}_{\text{reg}} = \boldsymbol{Q} + \alpha \ \text{diag}[\tau'_k I_m, \dots, \tau'_{k+N-1} I_m], \tag{28}$$

*the terms "*const.*",* $\tilde{\boldsymbol{Y}}$*,* $\boldsymbol{V}$*, and* $\boldsymbol{Q}$ *as in* (22), diag$[\cdot]$ *representing a diagonal block matrix whose input arguments are the matrices along the diagonal, and* I_m *denoting the identity over* $\mathbb{R}^m$*.*

Proof: Since the references are assumed to be ZOH, then the regularization term of (26) may be written as:

$$\|\boldsymbol{r}(t)\|^2_{0,[t_{k'}, t_{k'+N}]} = \boldsymbol{r}^\top \ \text{diag}[\tau_k I_m, \dots, \tau_{k+N-1} I_m] \boldsymbol{r}$$

The steps to reach (22) remain the same so that the modified cost can be written as:

$$\begin{aligned} J = \text{const.} &- 2(\tilde{\boldsymbol{Y}} - \boldsymbol{x}_0^\top \boldsymbol{V})\boldsymbol{r} \\ &+ \boldsymbol{r}^\top \boldsymbol{Q} \boldsymbol{r} + \boldsymbol{r}^\top \alpha \ \text{diag}[\tau'_k I_m, \dots, \tau'_{k+N-1} I_m] \boldsymbol{r} \end{aligned}$$

Finally, the two weighting matrices of the quadratic terms may be combined into a single matrix $\boldsymbol{Q}_{\text{reg}}$, defined in (28), completing the proof.

One upshot of Lemma 3 is that the steps to find the optimal references (24) and optimal cost (25) remain the same, effectively replacing $\boldsymbol{Q}$ with the modified matrix $\boldsymbol{Q}_{\text{reg}}$. Additionally, since $\boldsymbol{Q}$ is positive semi-definite and α, $\tau_k > 0$, then $\boldsymbol{Q}_{\text{reg}}$ is positive definite and then invertible. This means that, from (24), the solution $\boldsymbol{r}^*$ under reference regularization is unique and equal to

$$\boldsymbol{r}^* = \boldsymbol{Q}_{\text{reg}}^{-1} (\tilde{\boldsymbol{Y}}^\top - \boldsymbol{V}^\top \boldsymbol{x}_0).$$

6 Simulations

We explore the impact of aperiodic sampling on a two-dimensional double integrator controlled by a PD, with $\boldsymbol{x} = [p_x, v_x, p_y, v_y]^\top$ and $\boldsymbol{r} = [r_x, r_y]^\top$. Here, p_i is the position of the system in the $i = \{x, y\}$ direction, v_i is the corresponding velocity, and r_i is the corresponding reference position in i^{th} direction. Both x and y evolve independently of one another, and form a subspace $\boldsymbol{x}_{\text{sub}} = [p_i, v_i]^\top$, $\boldsymbol{r}_{\text{sub}} = r_i$ that evolve according to the subspace matrices A_{sub} and B_{sub}:

$$A_{\text{sub}} = \begin{bmatrix} 0 & 1 \\ -K_P & -K_D \end{bmatrix}, B_{\text{sub}} = \begin{bmatrix} 0 \\ K_P \end{bmatrix}. \tag{29}$$

In this simulation, the gains of the internal controller were set as $K_P = 2$ and $K_D = 3$. The full state vector $\boldsymbol{x}$, under control of the references $\boldsymbol{r}$, thus evolves according to (1) under the block matrices A_{sub} and B_{sub}:

$$A = \begin{bmatrix} A_{\text{sub}} & 0 \\ 0 & A_{\text{sub}} \end{bmatrix}, B = \begin{bmatrix} B_{\text{sub}} & 0 \\ 0 & B_{\text{sub}} \end{bmatrix}. \tag{30}$$

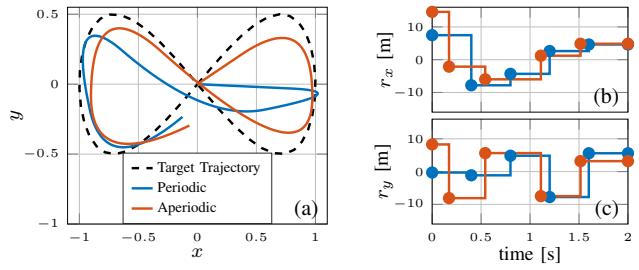

Fig. 3. Illustrating differences between periodic and aperiodic sampling.

Additionally, only the xy position of the system was tracked through the output, i.e., $\boldsymbol{y}(t) = [p_x(t), p_y(t)]^\top$. This means that in (1), we define:

$$C = \begin{bmatrix} 1 & 0 & 0 & 0 \\ 0 & 0 & 1 & 0 \end{bmatrix} \tag{31}$$

The aperiodic sampling time instants have been computed as described in Section 4.1, using a Particle Swarm Optimization (PSO) approach to implement the global optimization strategy invoked at line 10 of Algorithm 1.

Fig. 3 shows an example situation that highlights the difference between periodic and aperiodic sampling. The initial system state is $\boldsymbol{x}(0) = [0, 0, 0, 0]^\top$, with $\boldsymbol{y}(0) = [0, 0]^\top$.The dashed line of Fig. 3(a) shows the target trajectory $\tilde{\boldsymbol{y}}(t)$ defined as the following:

$$\tilde{y}(t) = \begin{bmatrix} \sin(2\pi t) \\ 0.5\sin(\pi t) \end{bmatrix} \tag{32}$$

Also shown in Fig. 3(a) is the result of optimal periodic sampling (blue) as well as optimal aperiodic sampling (orange), as determined by the PSO. For both periodic and aperiodic sampling, references were found over a horizon of 2 seconds, with $N = 5$, $\beta = 0$, and $\alpha = 5\text{e}{-4}$. These references are also shown in Fig. 3(b) and Fig. 3(c). Qualitatively, Fig. 3(a) shows how aperiodic reference sampling results in a trajectory that follows the target trajectory more closely than with periodic reference sampling.

To explore the effect of varying N, Fig. 4 shows the associated cost of both periodic and aperiodic reference sampling for different values of N. For a lower number of references, there exists a noticeable difference in cost between the two cases, illustrating how adding an extra degree of freedom (the sampling time of the references) affords a lower overall cost in the aperiodic sampling case. With larger N, however, more references control the system over the same time horizon, which has two effects: (i) the overall cost of both cases is lower, and (ii)

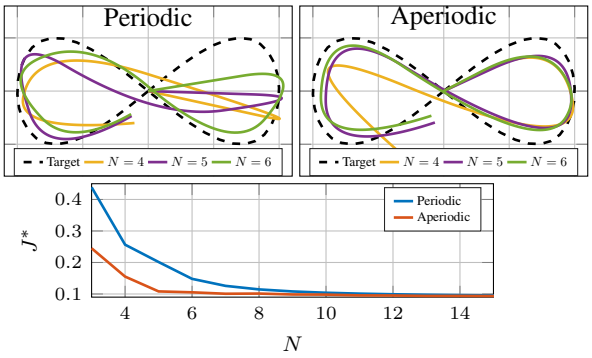

Fig. 4. Illustrating differences between periodic and aperiodic sampling.

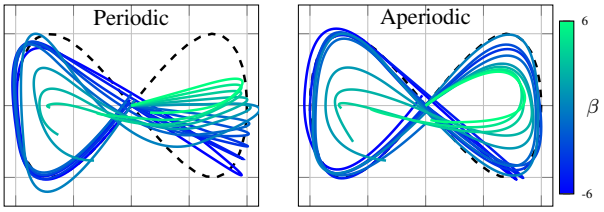

Fig. 5. Resulting trajectories from both periodic and aperiodic sampling with various values for β.

the difference in cost between both cases is also lower. For $N = 10$, the percentage difference between the periodic and aperiodic case is 0.6%, with virtually no difference for $N = 15$.

The effect of β is also explored in Fig. 5, showing resulting trajectories of both periodic and aperiodic sampling over a time horizon of 2 seconds for various values of $\beta \in [-6, +6]$. The target trajectory defined in (32) was again used, with $N = 5$. Qualitatively, increasing β results in the system trajectory more closely following the target trajectory for earlier times, whereas a lower β places more importance on tracking the later parts of the target trajectory.

7 Conclusion and Future Work

This paper presented an approach to optimally compute the discrete-time reference signal $\boldsymbol{r}_k$ given a desired continuous-time trajectory $\tilde{\boldsymbol{y}}(t)$ that the system output $\boldsymbol{y}(t)$ should follow. This approach was presented for the aperiodic sampling case and was investigated for its effects on the obtainable performance over different examples.

Future works involve investigating the impact of limited processing and communication capacity on the quality of the achieved control. Additional directions include the exploration of the impact of quantization, and the exploitation of past computations when calculating references in a receding horizon fashion.

Finally, we plan to apply the presented approach to additional use case applications, including experimental results in our evaluation, and further investigate its robustness against model uncertainty.

Acknowledgements

This work was supported by the Swedish Research Council (VR) with the PSI project (No. #2020-05094), by the Knowledge Foundation (KKS) with the MARC project (No. #20240011), by CoStar group, by DARPA under Contract No. FA8750-18-C-0090, by NSF under grant No. #1829004, and by the MAECI Italy-Sweden cooperation id. PGR02086.

References

Alur, R., Hristu-Varsakelis, D., Årzén, K., Levine, W., Baillieul, J., Henzinger, T., 2007. Handbook of Networked and Embedded Control Systems. Birkhäuser Boston.

Anderson, B.D., Moore, J.B., 2007. Optimal control: linear quadratic methods. Courier Corporation.

Bini, E., Buttazzo, G.M., 2014. The optimal sampling pattern for linear control systems. IEEE Trans. Automatic Control 59, 78–90.

Bini, E., Papadopoulos, A.V., Higgins, J., Bezzo, N., 2022. Optimal reference tracking for sampled-data control systems, in: IEEE 61st Annual Conf. Decision and Control (CDC), pp. 7141–7148.

Boyd, S., El Ghaoui, L., Feron, E., Balakrishnan, V., 1994. Linear matrix inequalities in system and control theory. SIAM, Philadelphia, PA.

Chen, T., Francis, B., 2012. Optimal Sampled-Data Control Systems. Communications and Control Engineering, Springer London.

Chen, T., Francis, B.A., 1995. Optimal Sampled-Data Control Systems. Springer-Verlag, London, UK.

Clerc, M., Kennedy, J., 2002. The particle swarm - explosion, stability, and convergence in a multidimensional complex space. IEEE Trans. Evolutionary Computation 6, 58–73.

Geromel, J.C., Colaneri, P., Bolzern, P., 2019. Differential linear matrix inequality in optimal sampled-data control. Automatica 100, 289–298.

Geromel, J.C., Souza, M., 2015. On an LMI approach to optimal sampled-data state feedback control design. Int. Journal of Control 88, 2369–2379.

Hara, S., Fujioka, H., Kabamba, P.T., 1994. A hybrid state-space approach to sampled-data feedback control. Linear Algebra and its Applications 205-206, 675–712.

Higgins, J., Bini, E., Bezzo, N., 2022. Offloaded receding horizon planning for environments with variable communication delays, in: IEEE Conf. Control Technology and Applications (CCTA).

Hildebrandt, C., Elbaum, S., Bezzo, N., Dwyer, M.B., 2020. Feasible and stressful trajectory generation for mobile robots, in: ACM SIGSOFT Int. Symp. Software Testing and Analysis, New York, NY, USA. p. 349–362.

Hwang, J.H., Arkin, R., Kwon, D.S., 2003. Mobile robots at your fingertip: Bezier curve on-line trajectory generation for supervisory control, in: IEEE/RSJ Int. Conf. Intelligent Robots and Systems (IROS), pp. 1444–1449.

Lau, B., Sprunk, C., Burgard, W., 2009. Kinodynamic motion planning for mobile robots using splines, in: IEEE/RSJ Int. Conf. Intelligent Robots and Systems (IROS), pp. 2427–2433.

Levis, A.H., Schlueter, R.A., Athans, M., 1971. On the behaviour of optimal linear sampled-data regulators. Int. Journal of Control 13, 343–361.

Liu, S., Sun, D., 2014. Minimizing energy consumption of wheeled mobile robots via optimal motion planning. IEEE/ASME Trans. Mechatronics 19, 401–411.

Mellinger, D., Kumar, V., 2011. Minimum snap trajectory generation and control for quadrotors, in: IEEE Int. Conf. robotics and automation, pp. 2520–2525.

Penicka, R., Scaramuzza, D., 2022. Minimum-time quadrotor waypoint flight in cluttered environments. IEEE Robotics and Automation Letters 7, 5719–5726.

Ragazzini, J., Franklin, G., 1958. Sampled-data Control Systems. McGraw-Hill, New York, NY.

Seron, M., Braslavsky, J., Goodwin, G., 2012. Fundamental Limitations in Filtering and Control. Communications and Control Engineering, Springer London.

Ugray, Z., Lasdon, L., Plummer, J., Glover, F., Kelly, J., Martí, R., 2007. Scatter search and local nlp solvers: A multistart framework for global optimization. INFORMS Journal on Computing 19, 328–340.

Wang, Z., Zhou, X., Xu, C., Chu, J., Gao, F., 2020. Alternating minimization based trajectory generation for quadrotor aggressive flight. IEEE Robotics and Automation Letters 5, 4836–4843.

Yang, Y., Long, P., Song, X., Pan, J., Zhang, L., 2021. Optimization-based framework for excavation trajectory generation. IEEE Robotics and Automation Letters 6, 1479–1486.